RESEARCH ARTICLE

Facile synthesis of bis-pentafluoroarylated anthracene derivatives for n-type organic field-effect transistor applications

Ryota Sato,[a] Takeshi Yasuda,[b] Takanobu Hiroto,[c] Takaki Kanbara,[a],* and Junpei Kuwabara[a],*

[a] Tsukuba Research Center for Energy Materials Science (TREMS), Graduate School of Pure and Applied Sciences, University of Tsukuba, 1-1-1 Tennodai, Tsukuba, Ibaraki 305-8573, Japan. E-mail: kanbara@ims.tsukuba.ac.jp kuwabara@ims.tsukuba.ac.jp
[b] Research Center for Functional Materials, National Institute for Materials Science (NIMS), 1-2-1 Sengen, Tsukuba, Ibaraki 305-0047, Japan.
[c] Research Network and Facility Services Division, National Institute for Materials Science (NIMS), 1-2-1 Sengen, Tsukuba, Ibaraki 305-0047, Japan

Supporting information for this article is given via a link at the end of the document.

Abstract: Diphenylanthracene (DPA) and its derivatives are promising semiconducting materials for p-type organic field-effect transistors (OFETs). In this study, to develop n-type semiconducting materials with an anthracene core, pentafluorobenzene was introduced into anthracene via C–H direct arylation, enabling the synthesis of various bis(pentafluorophenyl)anthracene (DPA-F) derivatives. The high reactivity of the pentafluorobenzene C–H bond allows direct arylation for synthesizing DPA-F derivatives in a single step. The introduction of strong electron-withdrawing pentafluorophenyl groups provides the anthracene derivatives with n-type semiconducting properties, in contrast to the p-type properties of the parent DPAs. Among the synthesized compounds, 2,6-bis(pentafluorophenyl)anthracene shows a high electron mobility of 0.12 ± 0.02 cm^2/Vs and an on/off ratio >10^6 in OFETs. The high crystallinity results in the smooth electron transport. This study provides a facile synthetic method for n-type semiconducting materials and insights into the molecular design of the positional effects of aromatic substituents on anthracene.

Introduction

Organic semiconducting materials are expected to emerge as the main materials in next-generation thin and lightweight device applications.[1] Various organic semiconducting materials have been developed as their molecular structures can be easily converted.[2] Among these materials, acene derivatives, which have a rigid conjugated backbone, exhibit high mobility in organic field-effect transistors (OFETs).[1–3] Owing to the inherent electron-rich characteristics of acene derivatives, they mostly serve as hole-transport materials (p-type) rather than electron-transport materials (n-type).[3] Diphenylanthracene (DPA) and its derivatives have been reported to exhibit excellent p-type semiconducting properties despite their easily accessible simple molecular structures.[4–8] Diphenylanthracene derivatives have also been applied in organic light-emitting transistors due to their high luminescence quantum yields.[4,6,7,9] In contrast, Yamashita et al. prepared anthracene with two 4-(trifluoromethyl)phenyl groups at the 2 and 6 positions.[10] This compound functioned as an n-type semiconductor with an OFET electron mobility (μ_e) of 3.4 × 10^{-3} cm^2/Vs and on/off ratio of >10^4 in vacuum at room temperature. However, the threshold voltage (V_{th}) is as high as 75 V. Additionally, as this compound was synthesized via the Suzuki–Miyaura coupling reaction, the synthetic method remains limited because of the large number of synthetic steps and low atom efficiency. To overcome these issues, we focused on direct arylation via C–H bond activation, which avoids the use of organometallic reagents for the synthesis of acene-based n-type semiconducting materials.[11–14] A pentafluorophenyl group was selected as the substituent owing to its strong electron-withdrawing characteristics, which is expected to provide n-type semiconducting properties.[15–17] For example, oligothiophene derivatives with two pentafluorophenyl groups at both ends can act as n-type semiconductors.[17] When pentafluorophenyl groups are introduced into anthracene, several regioisomers can be obtained.[18] The different positions of the pentafluorophenyl groups were expected to alter the torsion angles of the substituents and anthracene, thereby forming different molecular packing structures.[19] As the packing structures in the thin film are crucial factors for OFET performance, we aimed to clarify the effects of the positions of the pentafluorophenyl substituents on the molecular packing, physical properties, and device performance. To achieve this objective, we first established a facile synthetic protocol for regioisomers of bis(pentafluorophenyl)anthracene (DPA-F) derivatives using a direct arylation reaction. Among the synthesized compounds, 2,6-DPA-F shows a high μ_e of 0.12 ± 0.02 cm^2/Vs and an on/off ratio >10^6 in OFETs owing to high crystallinity.

Results and Discussion

First, we synthesized three DPA-F regioisomers (Scheme 1). 2,6-DPA-F was synthesized in a high yield (80%) via a direct arylation reaction under general reaction conditions (Scheme 1a).[20] Because the reaction of 1,5-dibromo anthracene with pentafluorobenzene was considered difficult owing to its steric hindrance,[18] we selected dicyclohexyl(2′,6′-dimethoxy[1,1′-biphenyl]-2-yl)phosphane (SPhos), which is a bulkier ligand than tris(*o*-methoxyphenyl)phosphine that facilitates a catalytic reaction (Scheme S1).[21] However, the reaction was incomplete, and the isolated yield of 1,5-DPA-F was low. Therefore, dicyclohexyl[2′,4′,6′-tris(propan-2-yl)[1,1′-biphenyl]-2-yl]phosphane (XPhos) was selected as a ligand to accelerate the catalytic reaction, particularly in the reductive elimination step, and the amounts of the Pd catalyst and ligand were also

increased to allow the reaction to proceed completely (Scheme 1b).[22] The modified reaction afforded 1,5-DPA-F in a 75% yield. The synthesis of the more sterically hindered 9,10-DPA-F[23] via direct arylation (Scheme S2) was more difficult. 9,10-DPA-F was obtained via a nucleophilic substitution reaction between anthraquinone and pentafluorophenyl lithium generated in situ and subsequent aromatization (Scheme 1c).[24] A derivative with a phenazine backbone instead of the anthracene skeleton was designed for comparison (Scheme 1d) because the introduction of nitrogen atoms generally leads to a deeper lowest unoccupied molecular orbital (LUMO) energy level, thereby reducing the electron injection barrier.[3,25–27] We attempted to synthesize 2,7-bis(pentafluorophenyl)phenazine (2,7-DPP-F) via the direct arylation of 2,7-dibromophenazine with pentafluorobenzene under XPhos-based reaction conditions. The reaction affords the target compound and a small amount of defluorinated byproduct (Scheme S3). Because the separation of the target compound from the byproduct is difficult, the optimization of the reaction conditions is required to avoid side reactions. We hypothesized that defluorination proceeded via the oxidative addition of a zerovalent Pd species to the sterically favored C–F bond of 2,7-DPP-F.[28,29] To avoid overreaction, the reaction was performed under mild conditions, and 2,7-DPP-F was obtained in 71% yield (Scheme 1d). Significantly, 2,7-DPP-F is a comparator substance for 2,6-DPA-F, although the numbers representing the positions are different owing to the nomenclature.

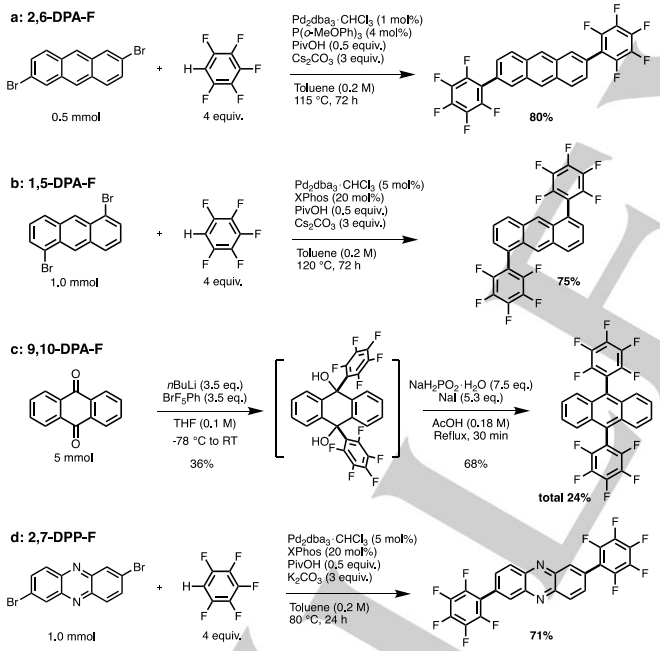

Scheme 1. Synthesis of DPA-F derivatives and 2,7-DPP-F.

The optical properties were measured to determine the effect of the substituent position on the fundamental physical properties. The absorption spectra of the DPA-F derivatives show two absorption bands at 370 and 260 nm (Figure 1a and Table S1). Long-wavelength absorptions at approximately 370 nm are observed in a similar wavelength range for all the DPA-F derivatives. In terms of short wavelength absorption, the absorption peaks of 2,6-DPA-F and 2,7-DPP-F are located on the longer-wavelength region than those of 1,5-DPA-F and 9,10-DPA-F. A time-dependent density-functional theory (TD-DFT) study was conducted to clarify the effects of the substituent positions on the conjugated system and their transitions.[30] The results show that the absorptions at approximately 370 nm are attributed to the highest occupied molecular orbital (HOMO)–LUMO transitions (Figure S2). In 2,7-DPP-F, HOMO-1 to LUMO transition contributes to the long-wavelength absorption in addition to the HOMO–LUMO transition. This overlapped absorption of 2,7-DPP-F is the origin of the broad absorption, which is in contrast to the absorption of the vibrational structures of other derivatives. The absorption at short wavelengths is mainly attributed to the transitions from HOMO to LUMO+1 in 2,6-DPA-F and 2,7-DPP-F. The corresponding LUMO+1 is delocalized over the entire molecule, including the pentafluorophenyl group (Figure S3). In contrast, the short-wavelength absorption of 1,5-DPA-F and 9,10-DPA-F is mainly attributed to transitions from HOMO-1 to LUMO. These molecular orbitals are localized on the anthracene core, presumably because of the limited conjugation between the anthracene core and pentafluorophenyl groups owing to the large torsion angles. The limited conjugation systems of 1,5-DPA-F and 9,10-DPA-F result in shorter-wavelength absorption. The emission spectra exhibit similar shapes for the DPA-F derivatives (Figure 1b). In contrast, the emission of 2,7-DPP-F is broad and negligible (Figure S1 and Table S1).

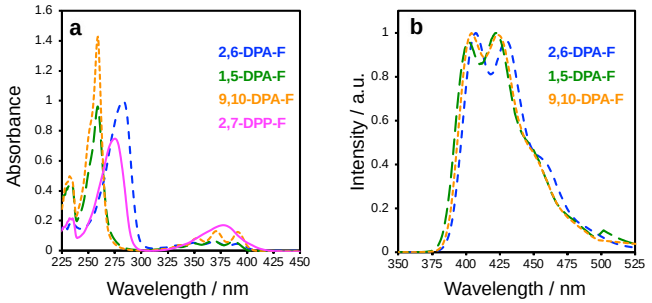

Figure 1. UV-vis absorption (a) and normarized emission (b) spectra of DPA-F derivatives in $CHCl_3$ (c = 1.0 x 10^{-5} M).

Subsequently, a single-crystal X-ray structural analysis was performed to confirm the structures and packing diagrams (Figures 2 and 3). The torsion angles between the central core and pentafluorophenyl group are strongly dependent on the position of the substituents and follows the order of 2,6-DPA-F (44°) < 2,7-DPP-F (49°) < 1,5-DPA-F (59°) < 9,10-DPA-F (86°) (Figure 2). The shortest C–C bond distance between the anthracene cores increases as the torsion angle increases (Figure 3).[1,31] The 2,6-DPA-F and 2,7-DPP-F distances are comparable to that of the parent 2,6-DPA (3.471 Å).[5] These results indicate that the position of the pentafluorophenyl groups affects the density of the packing structure.

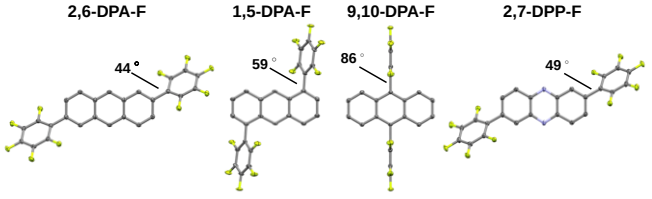

Figure 2. Crystal structures and torsion angles of DPA-F derivatives.

Out-of-plane X-ray diffraction (XRD) measurements of the vacuum-deposited films show similar patterns for 2,6-DPA-F and 2,7-DPP-F, confirming that these films have similar crystallinity and molecular orientations in the direction perpendicular to the substrate (Figure 4 and Table S2). The out-of-plane XRD patterns show the intense diffraction peaks of the 2,6-DPA-F and 2,7-DPP-

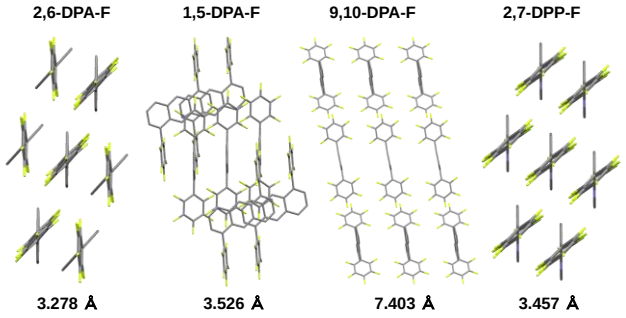

Figure 3. Molecular packing structures of DPA-F derivatives, obtained by the single X-ray structural analysis. Bottom numbers are the shortest carbon-carbon distances between anthracenes.

F films corresponding to the lattice spacing of 19 Å, which is close to the length of the molecules. Thus, 2,6-DPA-F and 2,7-DPP-F molecules are considered to be vertically oriented to the substrate in the film state. In contrast, weak peaks are observed in the XRD patterns of 1,5-DPA-F and 9,10-DPA-F, indicating their low crystallinity.[32] These results reveal that derivatives with small torsion angles form highly crystalline films via vapor deposition.[1,31] The HOMO energy levels were determined by photoelectron yield spectroscopy in the thin film state, and the LUMO energy levels were determined from the HOMO energy levels and band gaps from the absorption edge of the ultraviolet–visible (UV–vis) absorption spectra (Table 1 and Figures S4 and S5).[33,34] No significant differences are observed in the LUMO energy levels. All derivatives have deeper LUMO energy levels than those of 2,6-bis[4-(trifluoromethyl)phenyl]anthracene (-2.62 eV) reported by Yamashita et al.[10]

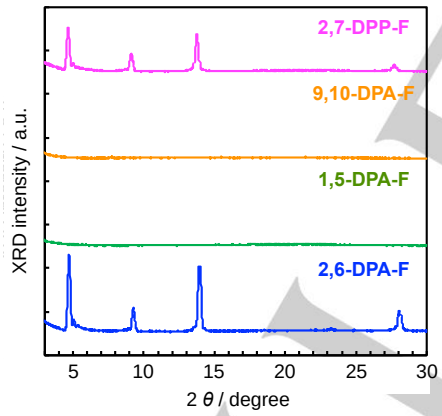

Figure 4. Out-of-plane XRD patterns of the vacuum-deposited film of DPA-F derivatives on the HMDS-treated SiO_2/Si substrate.

The n-type semiconducting characteristics of 2,6-DPA-F and 2,7-DPP-F, which form highly crystalline films, were evaluated (Table 2). The OFET with 2,6-DPA-F shows an μ_e of 0.12 ± 0.02 cm^2/Vs, an on/off ratio of > 10^6, and a V_{th} of 36 V (entry 1). 2,6-DPA-F has a higher μ_e and can be operated at a lower drive voltage than 2,6-bis[4-(trifluoromethyl)phenyl]anthracene (μ_e: 3.4 × 10^{-3} cm^2/V, on/off ratio: >10^4, and V_{th}: 75 V).[10] The OFET properties of 2,7-DPP-F were also evaluated using the same device configuration. Contrary to the expectation of a lower V_{th} owing to the nitrogen atoms,[3,25] 2,7-DPP-F shows a lower performance than 2,6-DPA-F in terms of μ_e, on/off ratio, and V_{th}. To discuss the differences in

Table 1. Physical properties of DPA-F derivatives in thin film.

molecule	λ_{Em} [nm]	PLQY [%]	λ_{edge} [nm]	$E_{g,opt}$ [eV]	HOMO [eV]	LUMO [eV]
2,6-DPA-F	413	21	415	2.99	-6.65	-3.66
1,5-DPA-F	433	12	411	3.02	-6.76	-3.74
9,10-DPA-F	412, 424	41	417	2.97	-6.60	-3.63
2,7-DPP-F	535	-[a]	425	2.92	-6.51	-3.59

[a] Less than 1%

the OFET performances between 2,6-DPA-F and 2,7-DPP-F, in-plane XRD measurements were performed to compare the in-plane crystallinity in the thin films. The in-plane XRD patterns (Figure S8 and Table S4) in contrast to almost the same out-of-plane XRD (Figure 4). This observation indicates that a crystal structure in the thin film state differs only in the in-plane direction. 2,6-DPA-F is expected to have an in-plane crystal structure suitable for carrier transport. Moreover, the XRD patterns of the 2,6-DPA-F film exhibit higher peak intensities and smaller full-width at half-maximum (FWHM) values of the obtained peaks than those of the 2,7-DPP-F film, suggesting the higher in-plane crystallinity of the 2,6-DPA-F film (Table S4). These results reveal that the high crystallinity in both the out-of-plane and in-plane directions in the 2,6-DPA-F film is the possible origin of the high OFET performance.[1,31] Additionally, the atomic force microscopy (AFM) image of the 2,6-DPA-F film shows a smooth surface compared to that of 2,7-DPP-F, which exhibits large aggregates (Figure S9). The smaller grain boundaries in the 2,6-DPA-F film may also contribute to its higher mobility.[35]

Table 2. Evaluation of DPA-F derivatives for FET[a].

entry	molecule	μ_e [cm^2/Vs]	on/off ratio	V_{th} [V]
1	2,6-DPA-F	0.12±0.02	>10^6	36±1
2	2,7-DPP-F	1.4±0.2 ×10^{-3}	>10^4	42±2

[a] Gate Si/HMDS treated SiO_2 insulator/evaporated film of molecule/source-drain Mg:Ag electrode.

Conclusion

In this study, we developed a facile method for introducing pentafluorophenyl groups into anthracenes via direct arylation. The optimization of the reaction conditions allows the synthesis of various DPA-F derivatives with different substitution positions in a single step. The substitution positions of the pentafluorophenyl groups strongly affect the morphology, crystallinity, and molecular orientation of the thin film. DPA-F bearing pentafluorophenyl groups at sterically vacant positions (2 and 6 positions) form a smooth thin film with high crystallinity and vertical molecular orientation packing, presumably because of the small torsion angles between the substituents and the anthracene core. These fundamental physical properties indicate that 2,6-DPA-F is a suitable structure for application in n-type semiconductors. Significantly, 2,6-DPA-F serves as an n-type organic

semiconductor in OFETs and exhibits an μ_e of 0.12 ± 0.02 cm^2/Vs and on/off ratio of $>10^6$.

Experimental Section

General, Measurement, and Materials.

^1H, ^{19}F, and $^{13}C\{^1H\}$ NMR spectra were recorded using Bruker AVANCE-400 NMR spectrometer and AVANCE-600 NMR spectrometer. Elemental analyses were carried out using a Perkin-Elmer 2400 CHN elemental analyzer and Yanaco CHN coder MT-6 or MT-5. Anhydrous toluene and THF were purchased from Kanto Chemical and used as dry solvents. Crystal Structure Determination Intensity data were collected on a Bruker SMART APEX II ULTRA with Mo Kα radiation. UV−vis absorption spectra in solution states were recorded on a Hitachi U-3900H spectrophotometer. Excitation and emission spectra in solution states were recorded on a Hitachi F-2700 fluorescence spectrophotometer. The PL quantum yields of the emission were measured using a Hamamatsu Photonics C9920-02 absolute PL quantum yield spectrometer. UV−vis absorption spectra and photoluminescence spectra for the vacuum-deposited films were recorded on a Hitachi U-3010 and JASCO FP-6500 spectrophotometer, respectively. The HOMO energy level was estimated by photoelectron yield spectroscopy (PYS) using a Riken Keiki AC-3 spectrometer. Out-of-plane and in-plane XRD measurements were performed using MiniFlex600 and SmartLab diffractometer (Rigaku Corporation, Cu Kα radiation), respectively. The incident angle ω was set to 0.3° for in-plane measurement.

Fabrication and characterization of OFETs.

To estimate the electron mobilities of the compounds, OFETs with a top-contact geometry were fabricated and characterized as follows. A SiO_2 insulator (300 nm) on Si substrate (gate electrode) was exposed to hexamethyldisilazane (HMDS) vapor. Vacuum-deposited films (40 nm) of the compounds were formed on the HMDS-treated SiO_2 layer. Mg:Ag (9:1 weight ratio) (80 nm)/Ag(40 nm) source-drain electrodes were thermally evaporated onto the substrates through shadow masks. The channel length and width were fixed at 75 μm and 5 mm, respectively. After fabricating the HMDS-treated SiO_2/Si substrate, OFETs were fabricated without exposure to air, and measured in a nitrogen atmosphere using a Keithley 2636A System Source Meter.

Acknowledgements

The authors thank the Chemical Analysis Center of the University of Tsukuba for the measurements of NMR, the single-crystal X-ray diffraction, and the elemental analysis. This work was partly supported by SEI GROUP CSR Foundation, JST A-STEP Grant Number JPMJTM20BT, and JST SPRING, Grant Number JPMJSP2124, JSPS KAKENHI Grant Number JP22J11647.

Keywords: anthracene • n-type semiconducting materials • polyfluoroarene • direct arylation • facile synthesis

[1] C. Wang, H. Dong, L. Jiang, W. Hu, *Chem. Soc. Rev.* **2018**, *47*, 422–500.

[2] C. Wang, H. Dong, W. Hu, Y. Liu, D. Zhu, *Chem. Rev.* **2012**, *112*, 2208–2267.

[3] A. N. Lakshminarayana, A. Ong, C. Chi, *J. Mater. Chem. C* **2018**, *6*, 3551–3563.

[4] J. Liu, H. Zhang, H. Dong, L. Meng, L. Jiang, L. Jiang, Y. Wang, J. Yu, Y. Sun, W. Hu, A. J. Heeger, *Nat. Commun.* **2015**, *6*, 10032.

[5] J. Liu, H. Dong, Z. Wang, D. Ji, C. Cheng, H. Geng, H. Zhang, Y. Zhen, L. Jiang, H. Fu, Z. Bo, W. Chen, Z. Shuai, W. Hu, *Chem. Commun.* **2015**, *51*, 11777–11779.

[6] K. Zhou, J. Liu, H. Dong, S. Ding, Y. Zhen, Y. Shi, W. Hu, *J. Mater. Chem. C* **2020**, *8*, 16333–11338.

[7] M. Chen, L. Yan, Y. Zhao, I. Murtaza, H. Meng, W. Huang, *J. Mater. Chem. C* **2018**, *6*, 7416–7444.

[8] M. Y. Vorona, N. J. Yutronkie, O. A. Melville, A. J. Daszczynski, S. Ovens, J. L. Brusso, B. H. Lessard, *Materials.* **2020**, *13*, 1961.

[9] Z. Qin, C. Gao, H. Gao, T. Wang, H. Dong, W. Hu, *Sci. Adv.* **2022**, *8*, eabp8775.

[10] S. Ando, J. Nishida, E. Fujiwara, H. Tada, Y. Inoue, S. Tokito, Y. Yamashita, *Chem. Mater.* **2005**, *17*, 1261–1264.

[11] D. Alberico, M. E. Scott, M. Lautens, *Chem. Rev.* **2007**, *107*, 174–238.

[12] D. J. Schipper, K. Fagnou, *Chem. Mater.* **2011**, *23*, 1594–1600.

[13] M. Lafrance, C. N. Rowley, T. K. Woo, K. Fagnou, *J. Am. Chem. Soc.* **2006**, *128*, 8754–8756.

[14] S. M. McAfee, G. C. Welch, *Chem. Rec.* **2019**, *19*, 989–1007.

[15] X. Gao, Y. Hu, *J. Mater. Chem. C* **2014**, *2*, 3099–3117.

[16] A. Facchetti, M. H. Yoon, C. L. Stern, H. E. Katz, T. J. Marks, *Angew. Chem. Int. Ed.* **2003**, *42*, 3900–3903.

[17] M. H. Yoon, A. Facchetti, C. E. Stern, T. J. Marks, *J. Am. Chem. Soc.* **2006**, *128*, 5792–5801.

[18] R. Sato, T. Iida, T. Kanbara, J. Kuwabara, *Chem. Commun.* **2022**, *58*, 11511–11514.

[19] T. Okamoto, K. Nakahara, A. Saeki, S. Seki, J. Hak Oh, H. B. Akkerman, Z. Bao, Y. Matsuo, *Chem. Mater* **2011**, *23*, 1646–1649.

[20] M. Wakioka, Y. Kitano, F. Ozawa, *Macromolecules* **2013**, *46*, 370–374.

[21] R. Martin, S. L. Buchwald, *Acc. Chem. Res.* **2008**, *41*, 1461–1473.

[22] T. E. Barder, S. L. Buchwald, *J. Am. Chem. Soc.* **2007**, *129*, 12003–12010.

[23] Y. Matsubara, A. Kimura, Y. Yamaguchi, Z. Yoshida, *Org. Lett.* **2008**, *10*, 5541–5544.

[24] K. Ono, H. Totani, T. Hiei, A. Yoshino, K. Saito, K. Eguchi, M. Tomura, J. Nishida, Y. Yamashita, *Tetrahedron* **2007**, *63*, 9699–9704.

[25] S. Kumagai, H. Ishii, G. Watanabe, C. P. Yu, S. Watanabe, J. Takeya, T. Okamoto, *Acc. Chem. Res.* **2022**, *55*, 660–672.

[26] W. G. GDillow, P. Kebarle, *Can. J. Chem.* **1989**, *67*, 1628–1631.

[27] Y. Takeda, P. Data, S. Minakata, *Chem. Commun.* **2020**, *56*, 8884–8894.

[28] M. I. Sladek, T. Braun, B. Neumann, H. G. Stammler, *J. Chem. Soc. Dalton Trans.* **2002**, 297–299.

[29] N. A. Jasim, R. N. Perutz, A. C. Whitwood, T. Braun, J. Izundu, B. Neumann, S. Rothfeld, H. G. Stammler, *Organometallics* **2004**, *23*, 6140–6149.

[30] S. Sasaki, K. Igawa, G. Konishi, *J. Mater. Chem. C* **2015**, *3*, 5940–5950.

[31] J. Li, K. Zhou, J. Liu, Y. Zhen, L. Liu, J. Zhang, H. Dong, X. Zhang, L. Jiang, W. Hu, *J. Am. Chem. Soc.* **2017**, *139*, 17261–17264.

[32] M. Y. Vorona, N. J. Yutronkie, O. A. Melville, A. J. Daszczynski, K. T. Agyei, S. Ovens, J. L. Brusso, B. H. Lessard, *Materials* **2019**, *12*, 2726.

[33] B. W. D'Andrade, S. Datta, S. R. Forrest, P. Djurovich, E. Polikarpov, M. E. Thompson, *Org. Electron.* **2005**, *6*, 11–20.

[34] P. I. Djurovich, E. I. Mayo, S. R. Forrest, M. E. Thompson, *Org. Electron.* **2009**, *10*, 515–520.

[35] S. W. Park, J. M. Hwang, J. M. Choi, D. K. Hwang, M. S. Oh, J. H. Kim, S. Im, *Appl. Phys. Lett.* **2007**, *90*, 88–91.

Entry for the Table of Contents

Insert graphic for Table of Contents here.

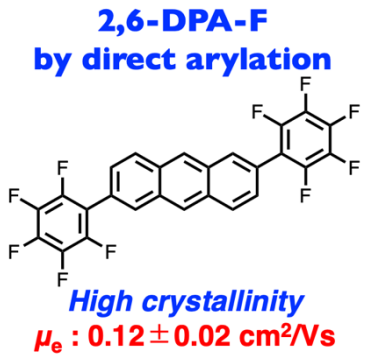

We demonstrated the introduction of two pentafluorophenyl groups into anthracene via direct C–H arylation. This facile method enabled the synthesis of various bis(pentafluorophenyl)anthracene derivatives with different substitution positions in a single step. Among them, 2,6-bis(pentafluorophenyl)anthracene (2,6-DPA-F) serves as an n-type semiconductor in OFETs, exhibiting an electron mobility of 0.12 ± 0.02 cm^2/V.